

Extraction of ND scattering lengths from the $\Lambda_b \rightarrow \pi^- p D^0$ decay and properties of the $\Sigma_c(2800)^+$

Shuntaro Sakai^a, Feng-Kun Guo^{a,b}, Bastian Kubis^c

^aCAS Key Laboratory of Theoretical Physics, Institute of Theoretical Physics, Chinese Academy of Sciences, Beijing 100190, China

^bSchool of Physical Sciences, University of Chinese Academy of Sciences, Beijing 100049, China

^cHelmholtz-Institut für Strahlen- und Kernphysik (Theorie) and Bethe Center for Theoretical Physics, Universität Bonn, 53115 Bonn, Germany

Abstract

The isovector and isoscalar ND s -wave scattering lengths are extracted by fitting to the LHCb data of the pD^0 invariant-mass distribution in the decay $\Lambda_b \rightarrow \pi^- p D^0$, making use of the cusp effect at the nD^+ threshold. The analysis is based on a coupled-channel nonrelativistic effective field theory. We find that the real part of the isovector ND scattering length is unnaturally large due to the existence of a near-threshold state with a mass around 2.8 GeV. The state is consistent with the $\Sigma_c(2800)^+$ resonance observed at Belle. Our results suggest that it couples strongly to the ND channel in an s -wave, and that its quantum numbers are $J^P = 1/2^-$. The strong cusp behavior at the nD^+ threshold can be verified using updated LHCb data.

Keywords: ND scattering lengths, charmed baryons

1. Introduction

Properties of the ND system have been paid much attention to as an analogue to the $\bar{K}N$ system, where there exists the $\Lambda(1405)$ resonance as a $\bar{K}N$ quasi-bound state near threshold [1–4] (for reviews, see Refs. [5, 6] and the review article dedicated to the $\Lambda(1405)$ in the Reviews of Particle Physics [7]). Several studies are devoted to the ND system from the viewpoint of the description of the Λ_c^* or Σ_c^* charmed baryons [8–22]. Some reactions concerning the ND system and Λ_c^* resonances have been investigated [23–25] and extensions to systems with D and nuclei performed (see, for example, Ref. [26] and references therein). Most of these studies discuss possible hadronic molecules (see Ref. [27] for a recent review) in the charmed-meson–nucleon systems, analogous to the XYZ states in the heavy-quarkonia mass region and the hidden-charm pentaquarks. However, relevant experimental information is scarce and the above-mentioned calculations are based on phenomenological models.

At low energies, the short-range interaction between two particles can be described by the effective-range ex-

pansion,¹

$$f_0^{-1}(k) = \frac{1}{a_0} + \frac{1}{2}r_0k^2 - ik + \mathcal{O}(k^4) \quad (1)$$

for s -waves, where $f_0(k)$ is the s -wave amplitude and k is the magnitude of the center-of-mass (c.m.) momentum. Threshold parameters, including the scattering length a_0 and the effective range r_0 , are important quantities as they govern the low-energy behavior of the scattering amplitude. Their values can be used to infer the structure of s -wave shallow bound states if there are any [27, 28].

It is well-known that in invariant-mass distributions there must be cusps exactly at two-body s -wave thresholds of opening channels due to unitarity. Because the masses of the involved particles are fixed, the cusp strength is then determined by the interaction at threshold, and thus threshold cusps can be used to extract the corresponding scattering lengths (we refer to Ref. [29] for a recent review on this topic). In the case of $\pi\pi$ scattering, the role of a cusp at the $\pi^+\pi^-$ threshold in the $\pi^0\pi^0$ spectrum was discussed in Refs. [30, 31], and a

¹The sign convention here is such that a positive (negative) scattering length corresponds to an attractive (repulsive) interaction in the absence of a bound-state pole. When there is a bound state below threshold, the scattering length is negative.

Email addresses: shsakai@itp.ac.cn (Shuntaro Sakai), fkguo@itp.ac.cn (Feng-Kun Guo), kubis@hiskp.uni-bonn.de (Bastian Kubis)

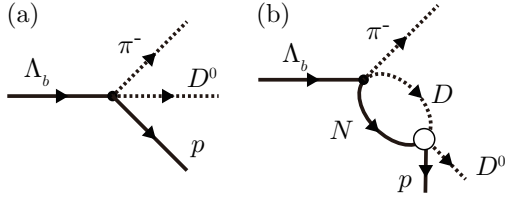


Figure 1: Diagrams for the decay $\Lambda_b \rightarrow \pi^- p D^0$ taken into account in this study. Here ND represents both pD^0 and nD^+ .

possible way to extract the $\pi\pi$ scattering length from the threshold cusp was suggested in Refs. [32, 33], followed by reformulations based on a nonrelativistic effective field theory (NREFT) [34, 35] (cf. also Ref. [36]). The difference between the $\pi\pi(I=0)$ and $\pi\pi(I=2)$ scattering lengths is tied to the magnitude of the $\pi^+\pi^-$ threshold cusp in the $\pi^0\pi^0$ distribution in the decays $K^\pm \rightarrow \pi^\pm\pi^0\pi^0$, and the $\pi\pi$ scattering lengths were determined from the cusp in the subsequent experimental studies [37, 38]. This framework was applied to other processes in Refs. [39–43]. In the present study, we try to extract the s -wave scattering lengths of the ND system from the pD^0 invariant-mass distribution of the decay $\Lambda_b \rightarrow \pi^- p D^0$ measured by the LHCb Collaboration [44], where a peculiar structure near the nD^+ threshold (about 6 MeV higher than the pD^0 threshold) is seen.

The Letter is organized as follows. In Sec. 2, the NREFT formalism is introduced that can be used in analyzing the pD^0 invariant-mass distribution in the near-threshold region. In Sec. 3, the results of fitting to the s -wave contribution extracted from the LHCb analysis are presented. A brief summary is given in Sec. 4.

2. Setup

In Fig. 1, we show the diagrams considered in this study. Diagram (a) of Fig. 1 represents the $\pi^- p D^0$ production from Λ_b without rescattering of particles, and diagram (b) takes into account the subsequent rescattering of $ND \rightarrow p D^0$ where ND represents both pD^0 and nD^+ .

First, we explain the ND scattering part. The $\pi\pi$ low-energy scattering is known to be rather weak due to chiral suppression; on the contrary, there is no suppression for the ND near-threshold interaction and it might be strong enough to generate a nearby pole. We employ the coupled-channel NREFT as developed in Refs. [45, 46], which is based on the Lippmann–Schwinger equation and is adequate to treat the ND scattering in the near-threshold region. There are two channels: pD^0 and

nD^+ . The nonrelativistic T -matrix is given by the Lippmann–Schwinger equation as [45, 46]

$$t_{ij} = \left[(1 - vG)^{-1}v \right]_{ij} = \frac{2\pi}{\det} \begin{pmatrix} \frac{1}{\mu_1} \left(-\frac{1}{a_{22}} + ip_2 \right) & -\frac{1}{a_{12} \sqrt{\mu_1 \mu_2}} \\ -\frac{1}{a_{12} \sqrt{\mu_1 \mu_2}} & \frac{1}{\mu_2} \left(-\frac{1}{a_{11}} + ip_1 \right) \end{pmatrix}_{ij}, \quad (2)$$

$$\det = \left(\frac{1}{a_{12}} \right)^2 - \left(\frac{1}{a_{11}} - ip_1 \right) \left(\frac{1}{a_{22}} - ip_2 \right), \quad (3)$$

where $i=1$ and 2 denote the pD^0 and nD^+ channels, respectively, μ_i denotes the reduced mass, and p_i is the nonrelativistic momentum of D (or N) in the ND c.m. frame,

$$p_i = \sqrt{2\mu_i(M_{ND} - M_i - m_i)}, \quad (4)$$

with M_{ND} being the ND invariant mass, and M_i (m_i) the mass of D^0 or D^+ (p or n). With the above expression, the momentum p_i is defined above threshold. Below threshold, it is analytically continued to $i\sqrt{2\mu_i(M_i + m_i - M_{ND})}$. The NREFT is based on an expansion in powers of the velocity of the particles in their c.m. frame. At the leading order of the NREFT, which is sufficient in the immediate vicinity of the thresholds given the current data quality, the spins of the involved particles do not need to be considered. The interaction kernel v is a matrix for constant contact terms (the next-to-leading order terms are of $\mathcal{O}(p_i^2/\mu_i^2)$), and G is a 2×2 diagonal matrix with the diagonal matrix element G_i given by the nonrelativistic two-body loop function,

$$G_i^\Lambda = \int^\Lambda \frac{d^3\mathbf{q}}{(2\pi)^3} \frac{2\mu_i}{\mathbf{q}^2 - p_i^2 - i\epsilon} = i\frac{\mu_i}{2\pi} p_i + \frac{\mu_i}{\pi^2} \Lambda \left[1 + \mathcal{O}\left(\frac{p_i^2}{\Lambda^2}\right) \right]. \quad (5)$$

The ultraviolet (UV) divergence in the loop integral is regularized using a three-momentum cutoff Λ . In Eq. (2), the cutoff dependence of the loop function G_i is absorbed by the interaction kernel v , and the resulting parameters a_{ij} are cutoff-independent (see Refs. [45, 46] for details). The ND scattering lengths can be expressed in terms of these parameters. The scattering length a_i in channel i is defined by the scattering amplitude at threshold as

$$a_i = \frac{\mu_i}{2\pi} t_{ii} \Big|_{M_{ND}=m_i+M_i}. \quad (6)$$

If the interaction is strong enough, a near-threshold pole of the T -matrix can be generated as a zero of the determinant defined in Eq. (3).

With the isospin phase convention

$$|D^+\rangle = -\left|I = \frac{1}{2}, I_z = \frac{1}{2}\right\rangle \quad (7)$$

and all other states taking a positive sign, the ND scattering amplitudes in the isospin basis and that in the particle basis are related to each other as

$$\begin{aligned} t_{ND(I=0)} &= \frac{1}{2} (t_{pD^0, pD^0} + t_{nD^+, nD^+} + 2t_{nD^+, pD^0}), \\ t_{ND(I=1)} &= \frac{1}{2} (t_{pD^0, pD^0} + t_{nD^+, nD^+} - 2t_{nD^+, pD^0}). \end{aligned} \quad (8)$$

Hence, the difference of the ND scattering lengths with $I = 0$ and $I = 1$ is proportional to t_{nD^+, pD^0} ,

$$t_{nD^+, pD^0} = \frac{1}{2} (t_{ND(I=0)} - t_{ND(I=1)}). \quad (9)$$

At the lower (pD^0) threshold, the T -matrix elements are

$$\begin{aligned} t_{11}^{\text{th}} &= \frac{2\pi}{\mu_1} \left(-\frac{1}{a_{22}} - \kappa \right) \left[\frac{1}{a_{12}^2} - \frac{1}{a_{11}} \left(\frac{1}{a_{22}} + \kappa \right) \right]^{-1} \\ &\equiv \frac{2\pi}{\mu_1} a_c \simeq \frac{2\pi}{\mu_1} \left[\frac{1}{a_{11}} - \frac{1}{a_{12}^2 (a_{11}^{-1} + \kappa)} \right]^{-1}, \\ t_{12}^{\text{th}} &= -\frac{2\pi}{\sqrt{\mu_1 \mu_2}} \frac{1}{a_{12}} \left[\frac{1}{a_{12}^2} - \frac{1}{a_{11}} \left(\frac{1}{a_{22}} + \kappa \right) \right]^{-1} \\ &\equiv \frac{2\pi}{\sqrt{\mu_1 \mu_2}} a_x \simeq -\frac{2\pi}{\sqrt{\mu_1 \mu_2}} \frac{a_{11}}{a_{12}} \left(\frac{a_{11}}{a_{12}^2} - \frac{1}{a_{11}} - \kappa \right)^{-1}, \end{aligned} \quad (10)$$

where $\kappa = \sqrt{2\mu_2\delta}$ with $\delta = m_n + M_{D^+} - m_p - M_{D^0}$. One sees that $\kappa = \mathcal{O}(\delta^{1/2})$. The parameters a_{ij} must be analytic in the involved hadron masses. Thus, the isospin breaking difference $a_{22} - a_{11}$ is of $\mathcal{O}(\delta)$, and we have neglected such a difference in Eq. (10). The more natural parameters are a_c and a_x instead of a_{11} and a_{12} . They are connected to the isoscalar and isovector scattering lengths as

$$\begin{aligned} a_c &= \frac{1}{2} (a_{ND(I=0)} + a_{ND(I=1)}), \\ a_x &= \frac{1}{2} (a_{ND(I=0)} - a_{ND(I=1)}). \end{aligned} \quad (11)$$

The parameters a_{11} and a_{12} can be expressed in terms of a_c and a_x :

$$a_{11} = \frac{a_c^2 - a_x^2}{a_c + a_x^2 \kappa}, \quad a_{12} = \frac{a_c^2 - a_x^2}{a_x(1 + a_c \kappa)}. \quad (12)$$

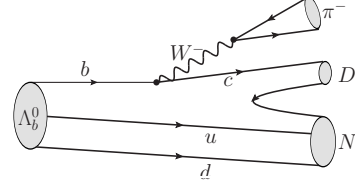


Figure 2: The W^- emission mechanism for the $\Lambda_b \rightarrow \pi^- pD^0$ decay.

Second, let us consider the production from the Λ_b decays. The leading contribution to the $\Lambda_b \rightarrow \pi^- ND$ decay in terms of the Cabibbo–Kobayashi–Maskawa matrix and color counting is the W^- emission mechanism, where the W^- boson emitted from the $b \rightarrow cW^-$ process becomes a π^- , see Fig. 2. Because the ud pair in the Λ_b is an isoscalar, the produced ND pair would be an isospin singlet as well. Thus, the production of the pD^0 should be approximately the same as that of the nD^+ .

Since parity is not conserved in the $\Lambda_b \rightarrow \pi^- ND$ weak decay, the ND pair can be produced not only in the s -wave, but also in higher partial waves. With the statistics of the current data, it is not possible to fix parameters with different partial waves included. Thus, we take the LHCb data and subtract the contributions from partial waves other than the ND s -wave. Several fits are presented in the LHCb analysis [44]. We take the analysis presented in Fig. 12 of Ref. [44], and subtract the contributions from the $J^P = 1/2^+$ and $3/2^+$ partial waves from the measured pD^0 invariant-mass distribution. In this way, only the $1/2^-$ part, corresponding to the ND s -wave, is left.

For the energy region close to the thresholds, the s -wave production can be approximated by a constant contact term followed by the final-state interaction (FSI). The ND FSI can be described by the non-relativistic T -matrix discussed above. Any possible singular behavior comes from the rescattering given in Eq. (2). We parametrize the s -wave contact term for the $\Lambda_b \rightarrow \pi^- ND$ production amplitude by a constant V_P . A momentum factor p_{π^-} associated with the W^- transition to π^- is absorbed into V_P as a constant because this factor is irrelevant to the nD^+ threshold cusp of interest, and we are focusing on a very small range of the ND invariant mass around the pD^0 and nD^+ thresholds.

Taking into account the ND rescattering described by Eq. (2) and the fact that ND produced from the Λ_b weak decay has $I = 0$, the decay amplitude of $\Lambda_b \rightarrow \pi^- pD^0$ in Fig. 1 for an ND s -wave can be written as follows:

$$\mathcal{A}_{s\text{-wave}} = V_P^\Lambda \left(1 + G_{pD^0}^\Lambda t_{pD^0, pD^0} + G_{nD^+}^\Lambda t_{nD^+, pD^0} \right), \quad (13)$$

where V_P has been rewritten as V_P^Λ to emphasize that it depends on the cutoff Λ . The second and third terms in the parentheses come from diagram (b) in Fig. 1 with s -wave ND rescattering. The rescattering of the other pairs (πN and πD) does not matter either because the pion moves much faster than the D -meson and the nucleon in the near- ND -threshold region. One notices that the T -matrix elements t_{pD^0,pD^0} and t_{nD^+,pD^0} are physical quantities and do not depend on the cutoff introduced in regularizing the UV divergence. The cutoff dependence of the loop functions in Eq. (13) needs to be absorbed by the production vertex V_P^Λ . Such a requirement is fulfilled by a multiplicative renormalization with $V_P \propto 1/\Lambda$ and by keeping only the leading-order term (in the expansion in powers of p_i/Λ) in the loop function in Eq. (5). Therefore, we find the following cutoff-independent amplitude:

$$\mathcal{A}_{s\text{-wave}} = V_P \left(t_{pD^0,pD^0} + t_{nD^+,pD^0} \right), \quad (14)$$

where V_P has been redefined to absorb the cutoff as well as other multiplicative constants with approximating $\mu_{pD^0} \simeq \mu_{nD^+}$ in the cutoff term of G_i^Λ . The procedure can be understood as that the process is dominated by the contribution from diagram (b) in Fig. 1.

Consequently, the $1/2^-$ part of the pD^0 invariant-mass distribution for the decay $\Lambda_b \rightarrow \pi^- pD^0$ can be fitted using

$$\frac{d\Gamma_{\Lambda_b \rightarrow \pi^- pD^0}}{dM_{pD^0}} = \mathcal{N} p_{\pi^- pD^0} \left| t_{pD^0,pD^0} + t_{nD^+,pD^0} \right|^2, \quad (15)$$

where \mathcal{N} is an overall normalization constant, $p_{\pi^- (pD^0)}$ is the momentum of the $\pi^- (D^0)$ in the $\Lambda_b (pD^0)$ rest frame.

The ND scattering lengths can be extracted by fitting to the $1/2^-$ partial wave of the pD^0 invariant-mass distribution reported in Ref. [44] using Eq. (15) as a fitting function. There is one more complexity due to the inelasticity from coupling pD^0 and nD^+ to lower channels such as $\pi\Lambda_c$ and $\pi\Sigma_c$. Since these channels are far away from the energy region of interest, the inelastic effects may be included by introducing imaginary parts to the parameters a_x and a_c . Unitarity is useful to constrain the parameter space: $\text{Im } t_{ii} = \sum_j \rho_j |t_{ij}|^2 \geq 0$ where $\rho_j \geq 0$ is the phase space factor of the intermediate states j . In order to obtain a stable fit, we further reduce the number of free parameters by approximating

$$\text{Im } a_x \simeq -\text{Im } a_c. \quad (16)$$

Considering that the phase space for the lowest two-body isovector channel $\pi\Lambda_c$ is larger than that for

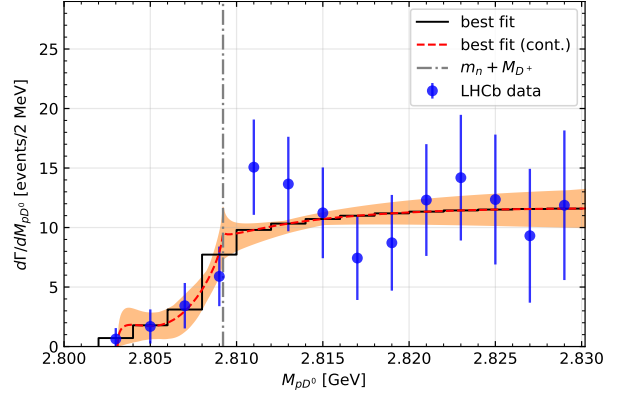


Figure 3: The best fit to the pD^0 distribution. The histogram shows the best fit with event numbers integrated in each bin, the dashed curve is the corresponding continuous distribution, which exhibit a clear cusp at the nD^+ threshold, and the band is the corresponding 1σ error region. The data points with error bars are taken from Fig. 12(b) in Ref. [44] with the contributions from the $J^P = 1/2^+$ and $3/2^\pm$ partial waves subtracted. The vertical dot-dashed line denotes the nD^+ threshold.

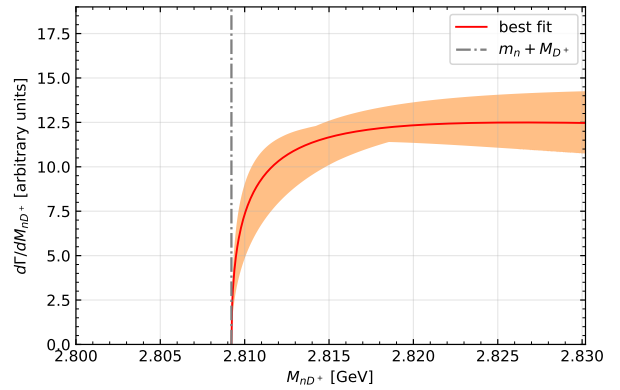


Figure 4: Prediction of the nD^+ distribution for the decay $\Lambda_b \rightarrow \pi^- nD^+$. The vertical dot-dashed line denotes the nD^+ threshold.

the isoscalar channel $\pi\Sigma_c$, it is reasonable to assume $\text{Im } a_{ND(I=0)} \ll \text{Im } a_{ND(I=1)}$. We therefore treat $\text{Im } a_{ND(I=0)}$ as a higher-order effect and neglect it in the leading approximation. This approximation is supported by the existing model calculations, listed in Table 2 below. Then Eq. (16) follows from Eq. (11). Hence, there are four free parameters in the fit, including $\text{Re } a_c$, $\text{Im } a_c$, $\text{Re } a_x$, and \mathcal{N} .

3. Results

As mentioned above, we subtract the $1/2^+$ and $3/2^\pm$ contributions from the pD^0 invariant-mass distribution of the $\Lambda_b \rightarrow \pi^- pD^0$ decay as reported in Fig. 12(b) in Ref. [44]. Using the MINUIT algorithm [47, 48], we

Table 1: Parameters from the best fit. The uncertainties are the 1σ errors propagated from the statistical uncertainties of the data.

Re a_c (GeV $^{-1}$)	Im a_c (GeV $^{-1}$)	Re a_x (GeV $^{-1}$)	\mathcal{N} (GeV 2)
$-11.7^{+4.5}_{-5.8}$	$6.8^{+4.0}_{-6.8}$	$7.7^{+4.7}_{-3.4}$	$0.04^{+0.06}_{-0.02}$

fit to the 14 data points below 2.83 GeV by averaging the function in Eq. (15) for each bin to take into account the binning of the measured pD^0 invariant-mass distribution.² Thus, the leading-order NREFT treatment is sufficient, given the large uncertainties of the current data set. In this range, the nonrelativistic treatment of the ND systems is well justified. The best fit has a reduced chi-square of $\chi^2/\text{dof} = 4.9/10$. In Fig. 3, the best fit to the $1/2^-$ partial wave of the pD^0 distribution is compared to the data. The measured distribution indeed shows an evident change around the nD^+ threshold despite the low statistics, and the best fit curve has a clear nD^+ threshold cusp. The resulting parameters from the fit are given in Table 1. We have checked that the values of a_c and a_x remain almost the same if we keep the loop functions in Eq. (13) and use Λ ranging from 0 to 10 GeV (the expression of G^Λ with $\Lambda = 0$ GeV is formally the same as the one using the $\overline{\text{MS}}$ scheme of dimensional regularization as one does in the studies of the $\pi\pi$ cusp in NREFT, see, e.g., Refs. [34, 35]). The change of Λ is absorbed by a corresponding change in the value of the normalization (V_p^2 effectively). Using the parameters from the fit, the nD^+ distribution for the decay $\Lambda_b \rightarrow \pi^- nD^+$ can be easily predicted, which is shown in Fig. 4.

The isoscalar and isovector ND scattering lengths obtained from the fit follow from Eq. (11), and are listed in Table 2, where the errors are the 1σ uncertainties propagated from the statistical errors of the data. For comparison, we also show the scattering lengths obtained in a few phenomenological models [10–12, 15] in Table 2. One sees that the results of the SU(4) DN model [11] and the meson-exchange model [15] are compatible with our findings.³

It is worthwhile to notice that the real parts of both

²The hard momentum scale of the NREFT considered here can be estimated as $\Lambda_{\text{hard}} = \sqrt{2\mu_i(M_{D^*} - M_D)} \approx 0.42$ GeV, which is the scale for the opening of the next relevant threshold, ND^* . At $M_{ND} = 2.83$ GeV, p_i^2/μ_i^2 is smaller than 0.09, meaning that the nonrelativistic expansion is well justified, and $p_i^2/\Lambda_{\text{hard}}^2$ is 0.19 for pD^0 and 0.15 for nD^+ , which is an estimate of the relative importance of the next-leading order contribution.

³The nD^0 scattering length is evaluated to be $-0.764 + i0.615$ fm

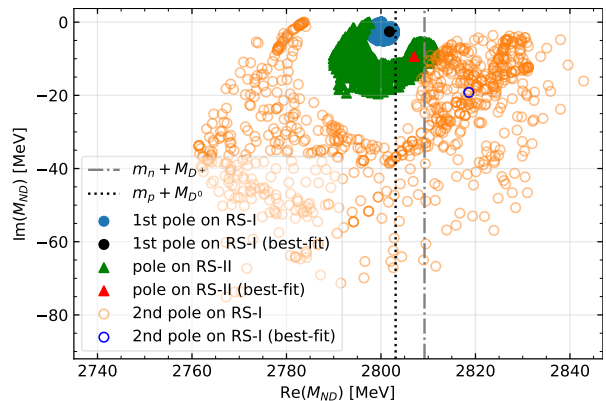


Figure 5: Poles in the first and second Riemann sheets using parameters in the 1σ range of the best fit.

the isoscalar and isovector scattering lengths are negative, meaning that the interaction in each channel is either repulsive or strongly attractive such that there is a bound state below threshold. The large absolute value of $\text{Re } a_{ND(I=1)}$ within errors suggests the existence of a near-threshold isovector bound state; in contrast, no strong conclusion can be made in the isoscalar sector: within the uncertainties, one can find a pole, which can be near threshold or too far away to be valid in the NREFT framework. Indeed, keeping isospin symmetry breaking, we find two poles in the first Riemann sheet (RS-I) of the complex M_{ND} plane⁴ for the T -matrix defined in Eq. (3), and one pole on the second Riemann sheet (RS-II). Their locations computed using about 1000 parameter sets within 1σ are shown in Fig. 5. For the first pole on RS-I, the absolute value of its residue to the isovector channel is at least more than 6 times (up to two orders of magnitude) larger than that to the isoscalar channel, except when the pole is located on the real axis, in which case the residue sizes are comparable. The pole on RS-II couples more strongly to the isovector than to the isoscalar channel, with the ratio of the residue size ranging from 1.6 to 3.8.⁵ These

in Ref. [49] (here the convention of the scattering length has been changed to be the same as ours), in which the parameters are chosen to reproduce the mass and width of the neutral $\Sigma_c(2800)$ measured by Belle [50].

⁴The first Riemann sheet is defined as the Riemann sheet with $\text{Im } p_1 > 0$ and $\text{Im } p_2 > 0$, and second Riemann sheet is defined as the one with $\text{Im } p_1 < 0$ and $\text{Im } p_2 > 0$. It is worthwhile to notice that because of the complexity of the $a_{11,12}$ parameters from the inelastic channels, there can be poles off the real axis on the first Riemann sheet, and the Schwarz reflection principle is not respected.

⁵In the isospin symmetric limit, there is only one isovector pole.

Table 2: The DN scattering lengths obtained from our fit in comparison with the results calculated in selected phenomenological models. The values for the SU(4) DN model [11] and the SU(8) DN model [12] are taken from Table 2 of Ref. [15], which considers a meson-exchange model. All values are given in units of fm.

a_{ND} [fm]	Our result	SU(4) [10]	SU(4) [11]	SU(8) [12]	Meson-exchange model [15]
$I = 0$	$-0.79^{+0.66}_{-0.61}$	-0.43	$-0.57 + i0.001$	$0.004 + i0.002$	$-0.41 + i0.04$
$I = 1$	$-3.8^{+1.4}_{-2.0} + i2.7^{+1.6}_{-2.7}$	-0.41	$-1.47 + i0.65$	$0.33 + i0.05$	$-2.07 + i0.57$

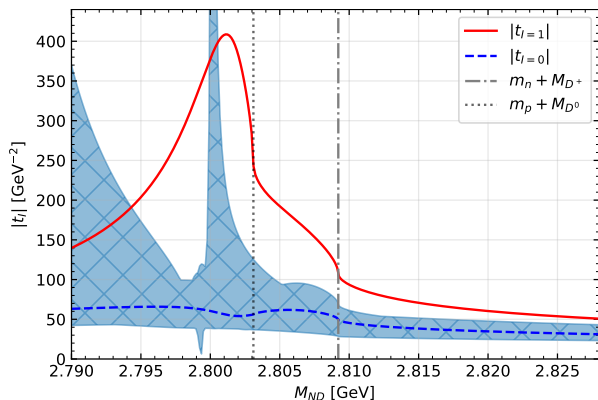


Figure 6: The absolute values of the isovector and isoscalar T -matrix elements from the best fit. The band is the 1σ uncertainty propagated from the data.

two poles are at:

$$\begin{aligned}
 \text{RS-I: } & 2801.8^{+1.0}_{-4.0} - i(2.6 \pm 2.6) \text{ MeV}, \\
 \text{RS-II: } & 2807.0^{+4.5}_{-17.1} - i(9.4^{+10.2}_{-9.4}) \text{ MeV}. \quad (17)
 \end{aligned}$$

From Fig. 6, one sees clearly that the 1st pole on RS-I produces a peak of $t_{I=1}$ below the pD^0 threshold, while the RS-II pole would be partly responsible for the ‘‘bump’’ between the pD^0 and nD^+ thresholds. The two poles could be assigned to the $\Sigma_c(2800)^+$ resonance discovered by the Belle Collaboration [50], which has a mass of 2792^{+14}_{-5} MeV and a width of 62^{+60}_{-40} MeV.⁶ Because of the isovector nature, the $\Sigma_c(2800)$ signal is much weaker than those of excited Λ_c states in the $\Lambda_b \rightarrow \pi^- pD^0$ decay. Yet, it leaves a footprint at the nD^0 threshold, producing a strong cusp. The threshold cusp effect can serve as a partial-wave filter since it shows up only for the s -wave. The quantum numbers of the $\Sigma_c(2800)$ are not known yet, and our analysis suggests them to be $J^P = 1/2^-$. This feature is shared

⁶Apart from the literature on the molecular interpretation of the $\Sigma_c(2800)$ cited in Sec. 1, studies related to the $\Sigma_c(2800)$ at the quark level can be found in, e.g., Refs. [51–61]. Concerning its spin and parity, no consensus has been reached so far.

by the results in a meson-exchange model in Ref. [15]. Yet, we notice that a recent study of $D^{(*)}N$ interaction using chiral effective field theory and model inputs for the involved low-energy constants did not find a bound state in the isovector ND system [22]. The analysis here should also be useful for improving the input of such studies.

In contrast, the second pole on RS-I couples dominantly to the isoscalar channel except when it is located on the real axis; furthermore, this pole in most of the parameter space is much further away from the thresholds, and one cannot make a unique conclusion on whether there is a near-threshold isoscalar pole (or even whether the isoscalar interaction is attractive or repulsive). Correspondingly, the curve for $|t_{I=0}|$ in most of the parameter space is quite smooth with two mild threshold cusps (as can be seen from the blue dashed best-fit curve in Fig. 6).

4. Summary

In this study, we have extracted the isoscalar and isovector ND scattering lengths from the pD^0 invariant-mass distribution for the $\Lambda_b \rightarrow \pi^- pD^0$ decay reported by the LHCb Collaboration [44]. In particular, there is a structure in the data around the nD^+ threshold that is likely due to the nD^+ threshold cusp. The strength of the cusp is sensitive to the ND interaction, and thus can shed light on resonances near the ND threshold. Our analysis is based on a low-energy nonrelativistic effective field theory with pD^0 and nD^+ coupled channels. The effects of lower channels are built in by introducing imaginary parts to the scattering lengths. From fitting to the $1/2^-$ partial wave of the pD^0 distribution, we find that the real parts of both the isoscalar and isovector ND scattering lengths are negative, implying that the interactions are either repulsive or have a bound state below threshold. Within uncertainties, the real part of the isoscalar ND scattering length ranges from -1.4 to -0.1 fm, and thus one is not able to conclude whether there must be a near-threshold isoscalar Λ_c excited state or the interaction

is repulsive. In contrast, the absolute value of the real part of the isovector ND scattering length is always large, indicating the existence of a bound-state pole below the pD^0 threshold. We indeed find a bound state at $2801.8_{-4.0}^{+1.0} - i(2.6 \pm 2.6)$ MeV; another pole in RS-II is found at $2807.0_{-17.1}^{+4.5} - i(9.4_{-9.4}^{+10.2})$ MeV. Both of them couple dominantly to the isovector channel, and in the isospin limit only one bound-state pole is left, suggesting they correspond to a two-pole structure of the same state due to coupled channels. This state could be assigned to the $\Sigma_c(2800)$ discovered by the Belle Collaboration [50], and its quantum numbers are suggested to be $J^P = 1/2^-$. Data with better statistics would be helpful to further clarify this situation.

Acknowledgements

F.-K.G. is grateful to Anton Poluektov for helpful communications. This work is supported in part by the National Natural Science Foundation of China (NSFC) and the Deutsche Forschungsgemeinschaft (DFG) through the funds provided to the Sino-German Collaborative Research Center CRC110 ‘‘Symmetries and the Emergence of Structure in QCD’’ (NSFC Grant No. 11621131001), by the NSFC under Grants No. 11835015, No. 11947302, and No. 11961141012, by the Chinese Academy of Sciences (CAS) under Grants No. XDB34030303 and No. QYZDB-SSW-SYS013, and by the CAS Center for Excellence in Particle Physics (CCEPP). S.S. is also supported by the 2019 International Postdoctoral Exchange Program, and by the CAS President’s International Fellowship Initiative (PIFI) under Grant No. 2019PM0108.

References

- [1] R. H. Dalitz, S. F. Tuan, The phenomenological description of K -nucleon reaction processes, *Annals Phys.* 10 (1960) 307–351. [doi:10.1016/0003-4916\(60\)90001-4](#).
- [2] N. Kaiser, P. B. Siegel, W. Weise, Chiral dynamics and the low-energy kaon-nucleon interaction, *Nucl. Phys.* A594 (1995) 325–345. [arXiv:nucl-th/9505043](#), [doi:10.1016/0375-9474\(95\)00362-5](#).
- [3] E. Oset, A. Ramos, Nonperturbative chiral approach to S -wave $\bar{K}N$ interactions, *Nucl. Phys.* A635 (1998) 99–120. [arXiv:nucl-th/9711022](#), [doi:10.1016/S0375-9474\(98\)00170-5](#).
- [4] J. A. Oller, U.-G. Meißner, Chiral dynamics in the presence of bound states: Kaon nucleon interactions revisited, *Phys. Lett.* B500 (2001) 263–272. [arXiv:hep-ph/0011146](#), [doi:10.1016/S0370-2693\(01\)00078-8](#).
- [5] T. Hyodo, D. Jido, The nature of the $\Lambda(1405)$ resonance in chiral dynamics, *Prog. Part. Nucl. Phys.* 67 (2012) 55–98. [arXiv:1104.4474](#), [doi:10.1016/j.ppnp.2011.07.002](#).
- [6] Y. Kamiya, K. Miyahara, S. Ohnishi, Y. Ikeda, T. Hyodo, E. Oset, W. Weise, Antikaon–nucleon interaction and $\Lambda(1405)$ in chiral SU(3) dynamics, *Nucl. Phys.* A954 (2016) 41–57. [arXiv:1602.08852](#), [doi:10.1016/j.nuclphysa.2016.04.013](#).
- [7] M. Tanabashi, et al., Review of Particle Physics, *Phys. Rev.* D98 (2018) 030001. [doi:10.1103/PhysRevD.98.030001](#).
- [8] M. F. M. Lutz, E. E. Kolomeitsev, On charm baryon resonances and chiral symmetry, *Nucl. Phys.* A730 (2004) 110–120. [arXiv:hep-ph/0307233](#), [doi:10.1016/j.nuclphysa.2003.10.012](#).
- [9] J. Hofmann, M. F. M. Lutz, Coupled-channel study of crypto-exotic baryons with charm, *Nucl. Phys.* A763 (2005) 90–139. [arXiv:hep-ph/0507071](#), [doi:10.1016/j.nuclphysa.2005.08.022](#).
- [10] M. F. M. Lutz, C. L. Korpa, Open-charm systems in cold nuclear matter, *Phys. Lett.* B633 (2006) 43–48. [arXiv:nucl-th/0510006](#), [doi:10.1016/j.physletb.2005.11.046](#).
- [11] T. Mizutani, A. Ramos, D mesons in nuclear matter: A DN coupled-channel equations approach, *Phys. Rev.* C74 (2006) 065201. [arXiv:hep-ph/0607257](#), [doi:10.1103/PhysRevC.74.065201](#).
- [12] C. García-Recio, V. K. Magas, T. Mizutani, J. Nieves, A. Ramos, L. L. Salcedo, L. Tolos, The s -wave charmed baryon resonances from a coupled-channel approach with heavy quark symmetry, *Phys. Rev.* D79 (2009) 054004. [arXiv:0807.2969](#), [doi:10.1103/PhysRevD.79.054004](#).
- [13] C. E. Jiménez-Tejero, A. Ramos, I. Vidaña, Dynamically generated open charmed baryons beyond the zero range approximation, *Phys. Rev.* C80 (2009) 055206. [arXiv:0907.5316](#), [doi:10.1103/PhysRevC.80.055206](#).
- [14] O. Romanets, L. Tolos, C. García-Recio, J. Nieves, L. L. Salcedo, R. G. E. Timmermans, Charmed and strange baryon resonances with heavy-quark spin symmetry, *Phys. Rev.* D85 (2012) 114032. [arXiv:1202.2239](#), [doi:10.1103/PhysRevD.85.114032](#).
- [15] J. Haidenbauer, G. Krein, U.-G. Meißner, L. Tolos, DN interaction from meson exchange, *Eur. Phys. J.* A47 (2011) 18. [arXiv:1008.3794](#), [doi:10.1140/epja/i2011-11018-3](#).
- [16] W.-H. Liang, T. Uchino, C.-W. Xiao, E. Oset, Baryon states with open charm in the extended local hidden gauge approach, *Eur. Phys. J.* A51 (2015) 16. [arXiv:1402.5293](#), [doi:10.1140/epja/i2015-15016-1](#).
- [17] T. F. Caramés, A. Valcarce, Multiquark contributions to charm baryon spectroscopy, *Phys. Rev.* D90 (2014) 014042. [arXiv:1507.08046](#), [doi:10.1103/PhysRevD.90.014042](#).
- [18] C. García-Recio, C. Hidalgo-Duque, J. Nieves, L. L. Salcedo, L. Tolos, Compositeness of the strange, charm, and beauty odd parity Λ states, *Phys. Rev.* D92 (2015) 034011. [arXiv:1506.04235](#), [doi:10.1103/PhysRevD.92.034011](#).
- [19] J. Hofmann, M. F. M. Lutz, D -wave baryon resonances with charm from coupled-channel dynamics, *Nucl. Phys.* A776 (2006) 17–51. [arXiv:hep-ph/0601249](#), [doi:10.1016/j.nuclphysa.2006.07.004](#).
- [20] Y. Dong, A. Faessler, T. Gutsche, V. E. Lyubovitskij, Charmed baryon $\Sigma_c(2800)$ as a ND hadronic molecule, *Phys. Rev.* D81 (2010) 074011. [arXiv:1002.0218](#), [doi:10.1103/PhysRevD.81.074011](#).
- [21] J.-R. Zhang, S -wave $D^{(*)}N$ molecular states: $\Sigma_c(2800)$ and $\Lambda_c(2940)^{+?}$, *Phys. Rev.* D89 (9) (2014) 096006. [arXiv:1212.5325](#), [doi:10.1103/PhysRevD.89.096006](#).
- [22] B. Wang, L. Meng, S.-L. Zhu, $D^{(*)}N$ interaction and the structure of $\Sigma_c(2800)$ and $\Lambda_c(2940)$ in chiral effective field theory, *Phys. Rev.* D 101 (2020) 094035. [arXiv:2003.05688](#), [doi:10.1103/PhysRevD.101.094035](#).

- [23] J. Haidenbauer, G. Krein, U.-G. Meißner, A. Sibirtsev, Charmed meson rescattering in the reaction $\bar{p}d \rightarrow D\bar{D}N$, *Eur. Phys. J. A37* (2008) 55–67. [arXiv:0803.3752](#), [doi:10.1140/epja/i2008-10602-x](#).
- [24] W.-H. Liang, M. Bayar, E. Oset, $\Lambda_b \rightarrow \pi^-(D_s^-)\Lambda_c(2595)$, $\pi^-(D_s^-)\Lambda_c(2625)$ decays and DN , D^*N molecular components, *Eur. Phys. J. C77* (2017) 39. [arXiv:1610.08296](#), [doi:10.1140/epjc/s10052-017-4602-6](#).
- [25] W.-H. Liang, E. Oset, Z.-S. Xie, Semileptonic $\Lambda_b \rightarrow \bar{\nu}_l\Lambda_c(2595)$ and $\Lambda_b \rightarrow \bar{\nu}_l\Lambda_c(2625)$ decays in the molecular picture of $\Lambda_c(2595)$ and $\Lambda_c(2625)$, *Phys. Rev. D95* (2017) 014015. [arXiv:1611.07334](#), [doi:10.1103/PhysRevD.95.014015](#).
- [26] L. Tolos, Charming mesons with baryons and nuclei, *Int. J. Mod. Phys. E22* (2013) 1330027. [arXiv:1309.7305](#), [doi:10.1142/S0218301313300270](#).
- [27] F.-K. Guo, C. Hanhart, U.-G. Meißner, Q. Wang, Q. Zhao, B.-S. Zou, Hadronic molecules, *Rev. Mod. Phys.* 90 (2018) 015004. [arXiv:1705.00141](#), [doi:10.1103/RevModPhys.90.015004](#).
- [28] S. Weinberg, Evidence that the deuteron is not an elementary particle, *Phys. Rev.* 137 (1965) B672–B678. [doi:10.1103/PhysRev.137.B672](#).
- [29] F.-K. Guo, X.-H. Liu, S. Sakai, Threshold cusps and triangle singularities in hadronic reactions, *Prog. Part. Nucl. Phys.* 112 (2020) 103757. [arXiv:1912.07030](#), [doi:10.1016/j.pnpnp.2020.103757](#).
- [30] P. Budini, L. Fonda, Pion-pion interaction from threshold anomalies in K^+ decay, *Phys. Rev. Lett.* 6 (1961) 419. [doi:10.1103/PhysRevLett.6.419](#).
- [31] U.-G. Meißner, G. Müller, S. Steininger, Virtual photons in SU(2) chiral perturbation theory and electromagnetic corrections to $\pi\pi$ scattering, *Phys. Lett. B406* (1997) 154–160, [Erratum: *Phys. Lett. B407* (1997) 454]. [arXiv:hep-ph/9704377](#), [doi:10.1016/S0370-2693\(97\)00666-7](#), [doi:10.1016/S0370-2693\(97\)00839-3](#).
- [32] N. Cabibbo, Determination of the $a_0 - a_2$ pion scattering length from $K^+ \rightarrow \pi^+\pi^0\pi^0$ decay, *Phys. Rev. Lett.* 93 (2004) 121801. [arXiv:hep-ph/0405001](#), [doi:10.1103/PhysRevLett.93.121801](#).
- [33] N. Cabibbo, G. Isidori, Pion-pion scattering and the $K \rightarrow 3\pi$ decay amplitudes, *JHEP* 03 (2005) 021. [arXiv:hep-ph/0502130](#), [doi:10.1088/1126-6708/2005/03/021](#).
- [34] G. Colangelo, J. Gasser, B. Kubis, A. Rusetsky, Cusps in $K \rightarrow 3\pi$ decays, *Phys. Lett. B638* (2006) 187–194. [arXiv:hep-ph/0604084](#), [doi:10.1016/j.physletb.2006.05.017](#).
- [35] J. Gasser, B. Kubis, A. Rusetsky, Cusps in $K \rightarrow 3\pi$ decays: a theoretical framework, *Nucl. Phys. B850* (2011) 96–147. [arXiv:1103.4273](#), [doi:10.1016/j.nuclphysb.2011.04.013](#).
- [36] E. Gámiz, J. Prades, I. Scimemi, $K \rightarrow 3\pi$ final state interactions at NLO in CHPT and Cabibbo’s proposal to measure $a_0 - a_2$, *Eur. Phys. J. C50* (2007) 405–422. [arXiv:hep-ph/0602023](#), [doi:10.1140/epjc/s10052-006-0201-7](#).
- [37] J. R. Batley, et al., Observation of a cusp-like structure in the $\pi^0\pi^0$ invariant mass distribution from $K^\pm \rightarrow \pi^\pm\pi^0\pi^0$ decay and determination of the $\pi\pi$ scattering lengths, *Phys. Lett. B633* (2006) 173–182. [arXiv:hep-ex/0511056](#), [doi:10.1016/j.physletb.2005.11.087](#).
- [38] J. R. Batley, et al., Determination of the S -wave $\pi\pi$ scattering lengths from a study of $K^\pm \rightarrow \pi^\pm\pi^0\pi^0$ decays, *Eur. Phys. J. C64* (2009) 589–608. [arXiv:0912.2165](#), [doi:10.1140/epjc/s10052-009-1171-3](#).
- [39] M. Bissegger, A. Fuhrer, J. Gasser, B. Kubis, A. Rusetsky, Cusps in $K_L \rightarrow 3\pi$ decays, *Phys. Lett. B659* (2008) 576–584. [arXiv:0710.4456](#), [doi:10.1016/j.physletb.2007.11.008](#).
- [40] C.-O. Gullström, A. Kupść, A. Rusetsky, Predictions for the cusp in $\eta \rightarrow 3\pi^0$ decay, *Phys. Rev. C79* (2009) 028201. [arXiv:0812.2371](#), [doi:10.1103/PhysRevC.79.028201](#).
- [41] B. Kubis, S. P. Schneider, The cusp effect in $\eta' \rightarrow \eta\pi\pi$ decays, *Eur. Phys. J. C62* (2009) 511–523. [arXiv:0904.1320](#), [doi:10.1140/epjc/s10052-009-1054-7](#).
- [42] T. Hyodo, M. Oka, Determination of the $\pi\Sigma$ scattering lengths from the weak decays of Λ_c , *Phys. Rev. C84* (2011) 035201. [arXiv:1105.5494](#), [doi:10.1103/PhysRevC.84.035201](#).
- [43] X.-H. Liu, F.-K. Guo, E. Epelbaum, Extracting $\pi\pi S$ -wave scattering lengths from cusp effect in heavy quarkonium dipion transitions, *Eur. Phys. J. C73* (2013) 2284. [arXiv:1212.4066](#), [doi:10.1140/epjc/s10052-013-2284-2](#).
- [44] R. Aaij, et al., Study of the D^0p amplitude in $\Lambda_b^0 \rightarrow D^0p\pi^-$ decays, *JHEP* 05 (2017) 030. [arXiv:1701.07873](#), [doi:10.1007/JHEP05\(2017\)030](#).
- [45] T. D. Cohen, B. A. Gelman, U. van Kolck, An effective field theory for coupled channel scattering, *Phys. Lett. B588* (2004) 57–66. [arXiv:nucl-th/0402054](#), [doi:10.1016/j.physletb.2004.03.020](#).
- [46] E. Braaten, M. Kusunoki, Factorization in the production and decay of the $X(3872)$, *Phys. Rev. D72* (2005) 014012. [arXiv:hep-ph/0506087](#), [doi:10.1103/PhysRevD.72.014012](#).
- [47] F. James, M. Roos, Minuit: A system for function minimization and analysis of the parameter errors and correlations, *Comput. Phys. Commun.* 10 (1975) 343–367. [doi:10.1016/0010-4655\(75\)90039-9](#).
- [48] iminuit team, iminuit – a python interface to minuit, <https://github.com/scikit-hep/iminuit>, accessed: 2018-03-05.
- [49] U. Raha, Y. Kamiya, S.-I. Ando, T. Hyodo, Universal physics of the few-body system of two neutrons and one flavored meson, *Phys. Rev. C98* (3) (2018) 034002. [arXiv:1708.03369](#), [doi:10.1103/PhysRevC.98.034002](#).
- [50] R. Mizuk, et al., Observation of an isotriplet of excited charmed baryons decaying to $\Lambda_c^+\pi$, *Phys. Rev. Lett.* 94 (2005) 122002. [arXiv:hep-ex/0412069](#), [doi:10.1103/PhysRevLett.94.122002](#).
- [51] L. A. Copley, N. Isgur, G. Karl, Charmed Baryons in a Quark Model with Hyperfine Interactions, *Phys. Rev. D20* (1979) 768, [Erratum: *Phys. Rev. D23*, 817(1981)]. [doi:10.1103/PhysRevD.23.817.3](#), [doi:10.1103/PhysRevD.20.768](#).
- [52] D. Pirjol, T.-M. Yan, Predictions for s wave and p wave heavy baryons from sum rules and constituent quark model. 1. Strong interactions, *Phys. Rev. D56* (1997) 5483–5510. [arXiv:hep-ph/9701291](#), [doi:10.1103/PhysRevD.56.5483](#).
- [53] W. Roberts, M. Pervin, Heavy baryons in a quark model, *Int. J. Mod. Phys. A23* (2008) 2817–2860. [arXiv:0711.2492](#), [doi:10.1142/S0217751X08041219](#).
- [54] H. Garcilazo, J. Vijande, A. Valcarce, Faddeev study of heavy baryon spectroscopy, *J. Phys. G34* (2007) 961–976. [arXiv:hep-ph/0703257](#), [doi:10.1088/0954-3899/34/5/014](#).
- [55] D. Ebert, R. N. Faustov, V. O. Galkin, Masses of excited heavy baryons in the relativistic quark model, *Phys. Lett. B659* (2008) 612–620. [arXiv:0705.2957](#), [doi:10.1016/j.physletb.2007.11.037](#).
- [56] X.-H. Zhong, Q. Zhao, Charmed baryon strong decays in a chiral quark model, *Phys. Rev. D77* (2008) 074008. [arXiv:0711.4645](#), [doi:10.1103/PhysRevD.77.074008](#).
- [57] C. Chen, X.-L. Chen, X. Liu, W.-Z. Deng, S.-L. Zhu, Strong decays of charmed baryons, *Phys. Rev. D75* (2007) 094017. [arXiv:0704.0075](#), [doi:10.1103/PhysRevD.75.094017](#).
- [58] T. Yoshida, E. Hiyama, A. Hosaka, M. Oka, K. Sadato, Spectrum of heavy baryons in the quark model, *Phys. Rev. D92* (11) (2015) 114029. [arXiv:1510.01067](#), [doi:10.1103/PhysRevD.92.114029](#).

- [59] H.-X. Chen, W. Chen, Q. Mao, A. Hosaka, X. Liu, S.-L. Zhu, P-wave charmed baryons from QCD sum rules, *Phys. Rev. D* 91 (2015) 054034. [arXiv:1502.01103](#), [doi:10.1103/PhysRevD.91.054034](#).
- [60] Z. Shah, K. Thakkar, A. Kumar Rai, P. C. Vinodkumar, Excited State Mass spectra of Singly Charmed Baryons, *Eur. Phys. J. A* 52 (10) (2016) 313. [arXiv:1602.06384](#), [doi:10.1140/epja/i2016-16313-9](#).
- [61] B. Chen, K.-W. Wei, X. Liu, T. Matsuki, Low-lying charmed and charmed-strange baryon states, *Eur. Phys. J. C* 77 (3) (2017) 154. [arXiv:1609.07967](#), [doi:10.1140/epjc/s10052-017-4708-x](#).